CrossMark

Reaction intermediates in the catalytic Gif-type oxidation from nuclear inelastic scattering

S. Rajagopalan[1] [ID] · T. Asthalter[2] · V. Rabe[3] ·
S. Laschat[3]

Abstract Nuclear inelastic scattering (NIS) of synchrotron radiation, also known as nuclear resonant vibrational spectroscopy (NRVS), has been shown to provide valuable insights into metal-centered vibrations at Mössbauer-active nuclei. We present a study of the iron-centered vibrational density of states (VDOS) during the first step of the Gif-type oxidation of cyclohexene with a novel trinuclear $Fe_3(\mu_3\text{-O})$ complex as catalyst precursor. The experiments were carried out on shock-frozen solutions for different combinations of reactants: $Fe_3(\mu_3\text{-O})$ in pyridine solution, $Fe_3(\mu_3\text{-O})$ plus Zn/acetic acid in pyridine without and with addition of either oxygen or cyclohexene, and $Fe_3(\mu_3\text{-O})$/Zn/acetic acid/pyridine/cyclohexene (reaction mixture) for reaction times of 1 min, 5 min, and 30 min. The projected VDOS of the Fe atoms was calculated on the basis of pseudopotential density functional calculations. Two possible reaction intermediates were identified as $[Fe^{(III)}(C_5H_5N)_2(O_2CCH_3)_2]^+$ and $Fe^{(II)}(C_5H_5N)_4(O_2CCH_3)_2$, yielding evidence that NIS (NRVS) allows to identify the presence of iron-centered intermediates also in complex reaction mixtures.

✉ T. Asthalter
t.asthalter@web.de

S. Rajagopalan
rajagopalan78@hotmail.com

[1] Materials Science Group, Indira Gandhi Centre for Atomic Research, Kalpakkam-603102, Tamil Nadu, India

[2] Institute of Physical Chemistry, Universität Stuttgart, 70569 Stuttgart, Germany

[3] Institute of Organic Chemistry, Universität Stuttgart, Pfaffenwaldring 55, 70569 Stuttgart, Germany

Springer

1 Introduction

Organometallic compounds are well-established tools in catalytic reactions, where the activity and selectivity of the active catalyst depends strongly on the choice of the central metal and the nature of the surrounding ligands. The understanding of non-heme enzymatic reactions, as well as the optimization of novel biomimetic catalysts, is strongly fostered by an understanding of the key reaction steps at the active centre.

Among those reactions that have been widely studied for the purpose of mimicking enzymatic activity, the Gif-reaction [1–3] (see scheme in Fig. 1) stands out as being designed for the purpose of emulating iron-containing enzymes, such as P450. The development of novel ligands aims at optimizing selectivity and turnover number.

In this article, we describe the characterization of two intermediates in a Gif-type catalysis reaction, using Mössbauer spectroscopy and nuclear inelastic scattering (NIS) of synchrotron radiation [4–6], supported by density-functional calculations. The catalyst used was a soluble iron complex obtained from a novel trinuclear $Fe_3(\mu_3\text{-O})$ complex as catalyst precursor [7, 8].

Investigations of bonding strengths are traditionally the domain of IR absorption (where data below $400\,cm^{-1}$ can only be obtained with high experimental effort owing to detector sensitivity limits) or Raman scattering. NIS, also known as NRVS in part of the literature [9], is a new method that monitors selectively the bonding around a resonant or Mössbauer nucleus. It has been shown to provide unique information about symmetry and bonding at the active centre of organometallic or enzymatic catalysts [10–13].

It is the aim of the present paper to identify the oxidation and spin states of the iron species involved in the above Gif-type reaction, using classical Mössbauer spectroscopy, and to subsequently find suggestions for the local structure (coordination sphere around the iron atom) in different reaction stages using NIS.

The paper is organized as follows. In Section 2, the sample preparation, the Mössbauer measurements, and the NIS experiments are summarized. The experimental results and their interpretation in light of the DFT calculations are presented and discussed in Section 3.

2 Experiments

2.1 Sample preparation

The catalyst precursor is a solid trinuclear complex, the synthesis and characterization of which is described in [7, 8]. The catalytic precursor was formed by a reaction of 2,6-diacylpyridine and $Fe(NO_3)_3$ in pyridine, where the acyl groups can have varying tether lengths between the carbonyl and pyridine moieties. For the present study, tether lengths of $n = 2$ and $n = 3$ were chosen.

The samples were prepared according to the scheme given in Table 1.

As some of the liquid samples are sensitive to air, they were prepared ex-situ and subsequently injected into the sample holder within a glove bag under nitrogen or helium gas.
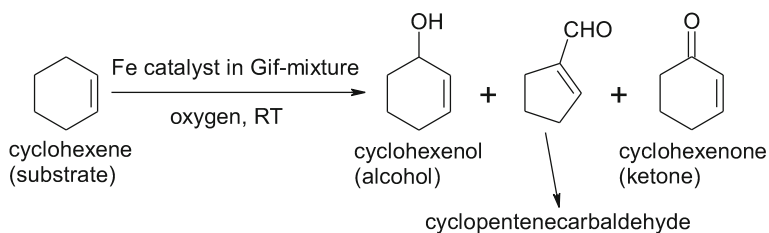
Fig. 1 Reaction scheme of the Gif-type reaction

The sample holder was then quickly dropped into liquid nitrogen and kept in frozen state until the experiment.

Whereas for the Mössbauer spectra, unenriched iron salts were used as educts, the starting material $Fe(NO_3)_3$ for the preparation of the trinuclear catalyst (and all solution samples) was prepared from iron powder enriched to 95.4 % in ^{57}Fe, purchased from Advanced Material Technologies Ltd. and used as received.

2.2 Mössbauer spectra

For the purpose of studying the reaction in solution, a set of liquid samples was prepared by dissolving the catalyst precursor in pyridine and adding various combinations of reactants according to the scheme given in Table 1. A drop of sample liquid was transferred into teflon sample holders having a cylindrical cross-section and shaped such that the sample liquid was confined to a flat disk of about 1 cm diameter and about 0.5 mm thickness.

The frozen samples were measured in a 4.2 K bath cryostat, using a gas proportional detector in transmission geometry and a ^{57}Co source in a rhodium matrix. Both the source and the sample were maintained at 4.2 K and the source followed a sinusoidal motion.

2.3 NIS experiment

In NIS experiments with synchrotron radiation, the energy of the incoming photons is scanned around the nuclear resonance energy (14.4125 keV in the case of the most popular isotope ^{57}Fe) within a range of typical phonon energies. The detuned photons can excite the resonant nuclei by creation (Stokes) or annihilation (Anti-Stokes) of one or more phonons or vibration quanta having the appropriate energy. After correcting for multi-phonon excitations, one obtains the VDOS associated with the root-mean-square displacement of the resonant nucleus.

The NIS experiments were carried out at the ID18 beamline of the European Synchrotron Radiation Facility using a high-resolution monochromator of the $+m, -n, -n, +m$ type [14, 15] (first pair of crystals: Si (4 4 0), second pair of crystals: Si (10 6 4)) yielding an overall energy resolution of about 1.0 meV (8 cm^{-1}) for the measurements at 70 K and 1.2 meV (9.6 cm^{-1}) for the measurements at 20 K and ensuring high spectral flux [16].

Copper or aluminium sample holders, coated with parylene-D so as to avoid corrosion by acetic acid and having kapton windows, were used. The frozen samples, preserved under liquid nitrogen, were quickly mounted onto the cold finger of the cryostat under a nitrogen gas stream, ensuring that the temperature did not exceed about 150 K during mounting (the melting point of pure pyridine being at 231 K).

Table 1 Overview of the samples studied by Mössbauer spectroscopy and NIS

Sample no.	Compounds	Remarks
1	trinuclear catalyst precursor	solid/powder
2	31.8 mg 1 dissolved in 0.9 ml pyridine	prepared in open atmosphere, then frozen for measurement
3	2 plus 0.07 ml acetic acid	”
4	3 plus 61 mg Zn powder	prepared and frozen under inert gas
5	4 flushed with O_2 gas	–
6	4 plus 0.05 ml cyclohexene	prepared and frozen under inert gas
7	reaction mixture after 1 min	reaction shown in Fig. 1
8	reaction mixture after 5 min	”
9	reaction mixture after 30 min	”

NIS measurements were performed at 20 K or 70 K and took about 8 to 12 h each. The synchrotron was operated in either 16-bunch (time window 176 ns) or hybrid mode, where the hybrid mode contained 24×8 bunches distributed over three quarters of the ring and a single bunch in the centre of the remaining quarter (leading to a time window of 352 ns). The extraction of the one-phonon contribution from the raw NIS spectra and the evaluation of the VDOS was carried out using DOS V2.1 [17].

2.4 Density-functional calculations

The geometry optimizations and subsequent frequency calculations in the harmonic approximation were carried out using the B3LYP hybrid exact-exchange functional [18, 19] as implemented in the GAUSSIAN03 package [20]. For the iron atom, the scalar-relativistic ECP pseudopotential was combined with the corresponding basis set for the Fe valence shells as described in [21]. Dunning's correlation-consistent polarized-valence double-zeta basis sets, which were augmented by diffuse functions, were used for the carbon, oxygen, nitrogen and hydrogen atoms [22].

For the calculation of the NIS spectra, use was made of the low-temperature approximation for powder samples [23, 24]

$$g(E) = \frac{1}{3} \sum_i e_i^2 = \frac{1}{3} \sum_i \frac{m_{\mathrm{Fe}} \left\langle u_{\mathrm{Fe},i}^2 \right\rangle}{\sum_k m_k \left\langle u_{k,i}^2 \right\rangle} \delta(E - E_i), \tag{1}$$

where m_{Fe} is the mass of the resonant Fe atom, $\left\langle u^2 \right\rangle$ is the mean-square displacement and i and k are summation indices for the i-th mode and the k-th atom in this mode, respectively. e_i^2 is also called the mode composition factor [24–26]. Finally, the normalization of each vibrational eigenvector with the square root of the reduced mass of the respective mode was taken into account when calculating the VDOS [23, 27]. In order to facilitate comparison with experiment, the resulting NIS spectra were convoluted with a Gaussian function possessing the resolution of the NIS experiment.
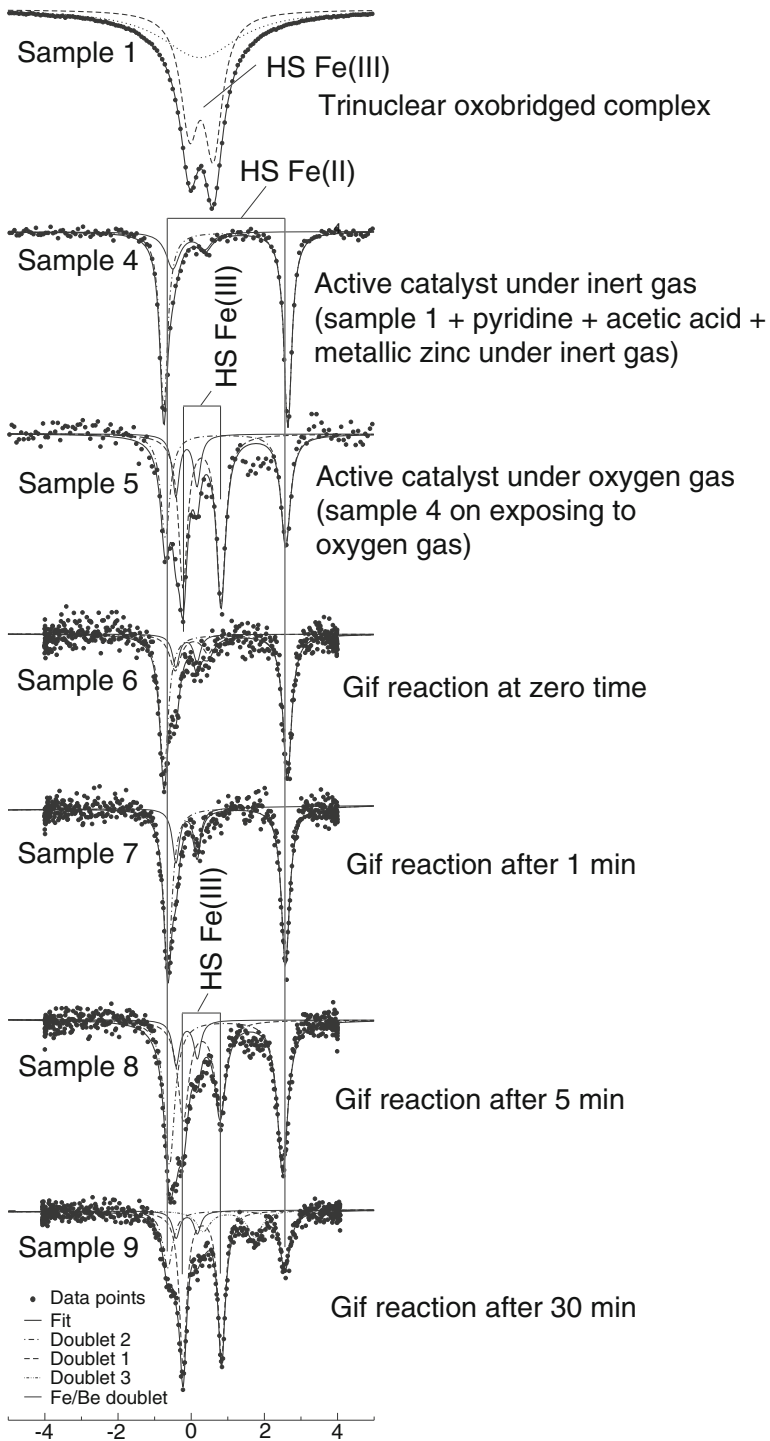
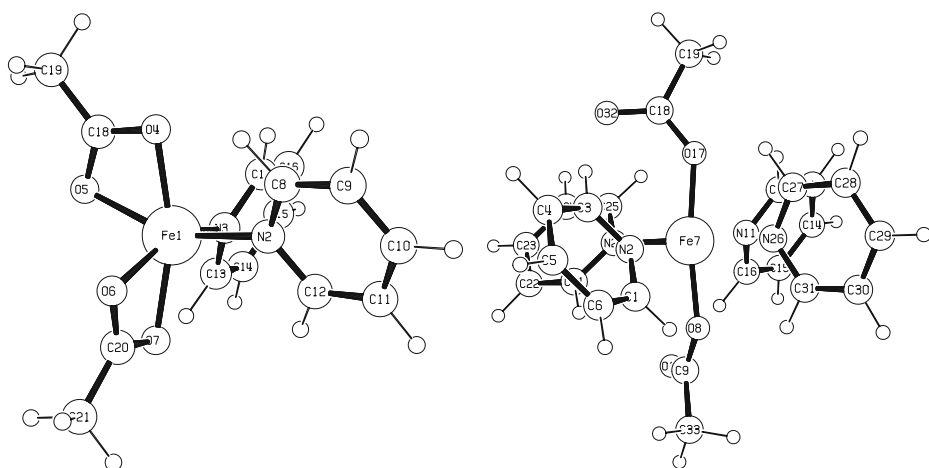**Fig. 2** Mössbauer spectra of frozen solutions of samples 1 and 4–9 (all at 4.2 K)

Fig. 3 Geometry optimized structure of the monomers; *left*: $[Fe^{(III)}(C_5H_5N)_2(O_2CCH_3)_2]^+$ (sample 3, monomer 1), *right*: $Fe^{(II)}(C_5H_5N)_4(O_2CCH_3)_2$ (sample 4, monomer 2)

3 Results and discussion

Figure 2 gives a comprehensive view of the Mössbauer spectra of samples 1 and 4 through 9, for tether length $n = 2$.

From a comparison of the Mössbauer parameters, the following findings can be deducted:

1. In the solid state, at 4.2 K the trinuclear catalyst precursor (sample 1) exhibits a typical high-spin Fe(III) doublet with an isomer shift of $\delta = (0.525 \pm 0.001)$ mm s^{-1} and a quadrupole splitting of $\Delta E_Q = (0.652 \pm 0.001)$ mm s^{-1}.
2. Under reducing Gif conditions in solution (sample 4), a high-spin Fe(II) doublet with an isomer shift of $\delta = (1.184 \pm 0.002)$ mm s^{-1} and a quadrupole splitting of $\Delta E_Q = (3.392 \pm 0.003)$ mm s^{-1} emerges. We attribute this doublet to a monomeric species that is identified with the active catalyst.
3. This doublet also dominates the spectra of samples 6 and 7 but its relative area decreases when the reaction proceeds (samples 8 and 9). This enables us to conclude that the active catalyst partly decomposes during the reaction.
4. Another doublet having an isomer shift of $\delta = (0.539 \pm 0.002)$ mm s^{-1} and a quadrupole splitting of $\Delta E_Q = (1.052 \pm 0.002)$ mm s^{-1} emerges during the reaction. This doublet is attributed to a newly formed high-spin Fe(III) species. Its isomer shift is somewhat smaller than the one of the trinuclear precursor, and its quadrupole splitting is considerably larger. We conclude that ligand exchange may have taken part within the first ligand sphere of the iron atom (decreased electron density at the nucleus $\rightarrow$ less shielding of the s electrons by the outer electrons) and that the Fe coordination sphere is more distorted with respect to a symmetrical octahedral geometry.

Samples 2 and 3 (not shown) exhibited complex non-Lorentzian line shapes, which are primarily due to paramagnetic relaxation effects of the Fe(III) ions (further details in [28]). We suggest that the added solvent partly enters the Fe ligand sphere, thus altering the
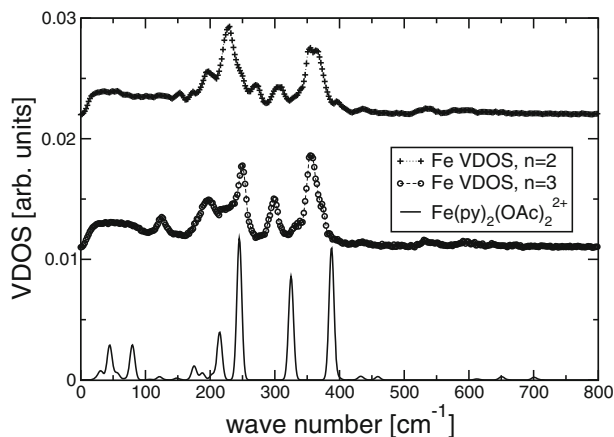
Fig. 4 Fe VDOS of sample 3 for trinuclear complexes with $n = 2$ and $n = 3$, together with the simulated VDOS for monomer 1 (Fig. 3, *left*)

electronic structure in the trimer, including the Fe-Fe spin coupling. As the spectra of samples 2 and 3 differ considerably, both pyridine and acetic acid are suggested to enter into the Fe coordination sphere. This gives us a first hint of a breaking-up of the trimer into monomers.

These findings are corroborated by the results of the NIS experiments. It is known from literature that possible intermediates involving the active centre of several non-heme enzymes using molecular oxygen are Fe monomers with either side-on or edge-on binding of two oxygen atoms [29], where the remaining coordination sites of iron are bonded to (solvent) ligands, and the Fe atom is in the Fe(III) high-spin state. Thus, in the present study, several monomers fulfilling these criteria were geometry-optimized, and their Fe VDOS was determined.

We first turn to the question what happens when acetic acid is added to the catalyst precursor (sample 3). The structure of the monomer ("monomer 1") that gave the best overall agreement with experiment is shown in Fig. 3 (left). Figure 4 shows the experimental ^{57}Fe VDOS of sample 3 together with the calculated VDOS of "monomer 1" ([$Fe^{(III)}(C_5H_5N)_2(O_2CCH_3)_2$]$^+$). A fair but not entirely convincing overall agreement between experiment and theory is observed.

Closer inspection reveals that the experimental spectra for $n = 2$ and $n = 3$ are slightly different. This immediately suggests that the structure presented in Fig. 3 (left) is not yet the correct structure but that at least one of the tethered pyridyl ligands that were present in the trinuclear complex might still bind to the Fe atom, e.g. in place of one of the acetyl groups. The high computational effort that is associated with geometry-optimizing and calculating the Fe VDOS of such a complex has precluded a corroboration so far.

We now contemplate the reduction step (sample 4). Again, several hypothetical structures were tested, and the one shown in Fig. 3 (right: "monomer 2") gave the most convincing results. Figure 5 shows the experimental ^{57}Fe VDOS of sample 4 together with the calculated VDOS of $Fe^{(II)}(C_5H_5N)_4(O_2CCH_3)_2$. In contrast to sample 3, here the two NIS spectra of the $n = 2$ and the $n = 3$ sample appear to be identical within the experimental accuracy. In other words, the Fe VDOS of the catalytically active complex appears not to
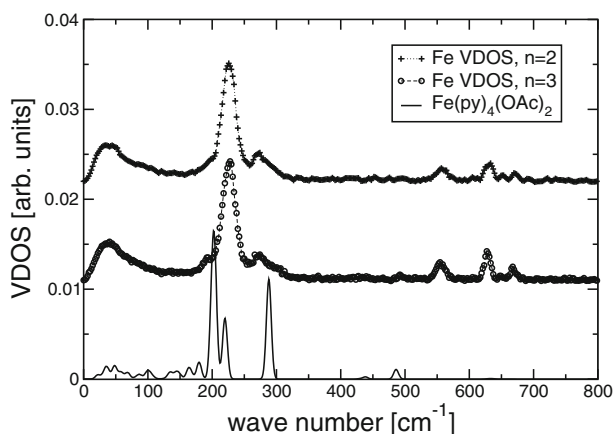
Fig. 5 Fe VDOS of sample 4 for trinuclear complexes with $n = 2$ and $n = 3$, together with the simulated VDOS for monomer 2 (Fig. 3, *right*)

depend on the tether length. This suggests that in the reduction step, the tethered pyridyl moiety might be entirely detached from the iron centre.

It should be noted that the calculated NIS spectra only take into account the experimental resolution and that the actual measured spectra are further broadened owing to inhomogeneities of the chemical environment caused by solvation. We further wish to emphasize that the DFT calculations are carried out on single molecules and hence neglect intermolecular interactions in solution. This may affect the quantitative agreement between experimental and calculated vibration spectra.

4 Conclusions

In the present study, we have demonstrated that NIS on frozen solutions of reaction intermediates appearing during catalysis yields valuable information about the local binding at the central, Mössbauer-active metal. Given the recent progresses that have been reported on iron-based catalysts [30], we anticipate that NIS may be a valuable tool to gain mechanistic insight into the associated reaction mechanisms.

References

1. Barton, D.H.R., Motherwell, R.S.H., Motherwell, W.B.: Further studies on the activation of the C–H bond in saturated hydrocarbons. Tetrahedron Lett. **24**, 1979 (1983)

2. Barton, D.H.R., Doller, D.: The selective functionalization of saturated hydrocarbons: Gif chemistry. Acc. Chem. Rec. **25**, 504 (1992)

3. Barton, D.H.R., Hu, B.: The functionalization of saturated hydrocarbons. Part 35. On the intermediates in an Fe-III catalase model in pyridine. Relevance to the catalase enzyme. Tetrahedron **52**, 10313 (1996)

4. Seto, M., Yoda, Y., Kikuta, S., Zhang, X.W., Ando, M.: Observation of nuclear resonant scattering accompanied by phonon excitation using synchrotron radiation. Phys. Rev. Lett. **74**, 3828 (1995)

5. Sturhahn, W., Toellner, T.S., Alp, E.E., Zhang, X., Ando, M., Yoda, Y., Kikuta, S., Seto, M., Kimball, C.W., Dabrowski, B.: Phonon density of states measured by inelastic nuclear resonant scattering. Phys. Rev. Lett. **74**, 3832 (1995)

6. Chumakov, A.I., Sturhahn, W.: Experimental aspects of inelastic nuclear resonance scattering. Hyperfine Interact **123/124**, 781 (1999)

7. Rabe, V.: Neue Nicht-Häm-Eisenkomplexe: Synthese, spektroskopische Charakterisierung und Anwendung in der katalytischen aeroben C-H-Oxidation, Dissertation, Universität Stuttgart (2009)

8. Rabe, V., Frey, W., Baro, A., Laschat, S., Bauer, M., Bertagnolli, H., Rajagopalan, S., Asthalter, T., Roduner, E., Dilger, H., Glaser, T., Schnieders, D.: Syntheses, crystal structures, spectroscopic properties, and catalytic aerobic oxidations of novel trinuclear non-heme iron complexes. Eur. J. Inorg. Chem. **2009**, 4660 (2009)

9. Smith, M.C., Xiao, Y., Wang, H., George, S.J., Coucouvanis, D., Koutmos, M., Sturhahn, W., Alp, E.E., Zhao, J., Cramer, S.P.: Normal-Mode Analysis of $FeCl_4^-$ and $Fe_2S_2Cl_4^{2-}$ via Vibrational Mössbauer, Resonance Raman, and FT-IR Spectroscopies. Inorg. Chem. **44**, 5562 (2005)

10. Bergmann, U., Sturhahn, W., Linn, D.E. Jr., Jenney, F.E. Jr., Adams, M.W.W., Rupnik, K., Hales, B.J., Alp, E.E., Mayse, A., Cramer, S.P.: Observation of Fe-H/D modes by nuclear resonant vibrational spectroscopy. J. Am. Chem. Soc. **125**, 4016 (2003)

11. Xiao, Y., Fisher, K., Smith, M.C., Newton, W.E., Case, D.A., George, S.J., Wang, H., Sturhahn, W., Alp, E.E., Zhao, J., Yoda, Y., Cramer, S.P.: How nitrogenase shakes - initial information about p-cluster and FeMo-cofactor normal modes from nuclear resonance vibrational spectroscopy (NRVS). J. Am. Chem. Soc. **128**, 7608 (2006)

12. Petrenko, T., George, S.D., Alcalde, N.A., Bill, E., Mienert, B., Xiao, Y., Guo, Y., Sturhahn, W., Cramer, S.P., Wieghardt, K., Neese, F.: Characterization of a genuine iron(V)-nitrido species by nuclear resonant vibrational spectroscopy coupled to density functional calculations. J. Am. Chem. Soc. **129**, 11053 (2007)

13. Leu, B.M., Ching, T.H., Zhao, J., Sturhahn, W., Alp, E.E., Sage, J.T.: Vibrational dynamics of iron in cytochrome c. J. Phys. Chem. B **113**, 2193 (2009)

14. Yabashi, M., Tamasaku, K., Kikuta, S., Ishikawa, T.: X-ray monochromator with an energy resolution of 810^{-9} at 14.41 keV. Rev. Sci. Instrum. **72**, 4080 (2001)

15. Chang, S.-L., Stetsko, Y.P., Tang, M.-T., Lee, Y.-R., Sun, W.-H., Yabashi, M., Ishikawa, T.: X-Ray resonance in crystal cavities: Realization of Fabry-Perot resonator for hard X Rays. Phys. Rev. Lett. **94**, 174801 (2005)

16. Chumakov, A.I.: Personal communication

17. Kohn, V.G., Chumakov, A.I.: DOS: Evaluation of phonon density of states from nuclear resonant inelastic absorption. Hyperfine Interact **125**, 205 (2000)

18. Lee, C., Yang, W., Parr, R.G.: Development of the Colle-Salvetti correlation-energy formula into a functional of the electron density. Phys. Rev. B **37**, 785 (1988)

19. Becke, A.D.: Density-functional thermochemistry. III. The role of exact exchange. J. Chem. Phys. **98**, 5648 (1993)

20. Frisch, M.J., Trucks, G.W., Schlegel, H.B., Scuseria, G.E., Robb, M.A., Cheeseman, J.R., Montgomery, J.A. Jr., Vreven, T., Kudin, K.N., Burant, J.C., Millam, J.M., Iyengar, S.S., Tomasi, J., Barone, V., Mennucci, B., Cossi, M., Scalmani, G., Rega, N., Petersson, G.A., Nakatsuji, H., Hada, M., Ehara, M., Toyota, K., Fukuda, R., Hasegawa, J., Ishida, M., Nakajima, T., Honda, Y., Kitao, O., Nakai, H., Klene, M., Li, X., Knox, J.E., Hratchian, H.P., Cross, J.B., Bakken, V., Adamo, C., Jaramillo, J., Gomperts, R., Stratmann, R.E., Yazyev, O., Austin, A.J., Cammi, R., Pomelli, C., Ochterski, J.W., Ayala, P.Y., Morokuma, K., Voth, G.A., Salvador, P., Dannenberg, J.J., Zakrzewski, V.G., Dapprich, S., Daniels, A.D., Strain, M.C., Farkas, O., Malick, D.K., Rabuck, A.D., Raghavachari, K., Foresman, J.B., Ortiz, J.V., Cui, Q., Baboul, A.G., Clifford, S., Cioslowski, J., Stefanov, B.B., Liu, G., Liashenko, A., Piskorz, P., Komaromi, I., Martin, R.L., Fox, D.J., Keith, T., Al-Laham, M.A., Peng, C.Y., Nanayakkara, A., Challacombe, M., Gill, P.M.W., Johnson, B., Chen, W., Wong, M.W., Gonzalez, C., Pople, J.A.: Gaussian 03, Revision E.01. Gaussian, Inc., Wallingford (2004)

21. Dolg, M., Wedig, U., Stoll, H., Preuss, H.: Energy-adjusted ab initio pseudopotentials for the first row transition elements. J. Chem. Phys. **86**, 866 (1987)

22. Dunning, T.H. Jr.: Gaussian basis sets for use in correlated molecular calculations. I. The atoms boron through neon and hydrogen. J. Chem. Phys. **90**, 1007 (1989)
23. Paulsen, H., Winkler, H., Trautwein, A.X., Grünsteudel, H., Rusanov, V., Toftlund, H.: Measurement and simulation of nuclear inelastic-scattering spectra of molecular crystals. Phys. Rev. B **59**, 975 (1999)
24. Chumakov, A.I., Rüffer, R., Leupold, O., Sergueev, I.: Insight to dynamics of molecules with nuclear inelastic scattering. Struct. Chem. **14**, 109 (2003)
25. Sage, J.T., Durbin, S.M., Sturhahn, W., Wharton, D.C., Champion, P.M., Hession, P., Sutter, J., Alp, E.E.: Long-range reactive dynamics in myoglobin. Phys. Rev. Lett. **86**, 4966 (2001)
26. Sage, J.T., Paxson, C., Wyllie, G.R.A., Sturhahn, W., Durbin, S.M., Champion, P.M., Alp, E.E., Scheidt, W.R.: Nuclear resonance vibrational spectroscopy of a protein active-site mimic. J. Phys. Condens. Matter **13**, 7707 (2001)
27. Asthalter, T.: Nuclear inelastic scattering on ferrocene-based rotator phases: Theory vs. experiment. Z. Phys. Chem. **220**, 979 (2006)
28. Rajagopalan, S.: Mössbauer spectroscopy, nuclear inelastic scattering and density functional theory studies on oxobridged iron complexes and their reaction under Gif-type conditions, Dissertation, Universität Stuttgart (2010)
29. Karlsson, A., Parales, J.V., Parales, R.E., Gibson, D.T., Eklund, H., Ramaswamy, S.: Crystal structure of naphthalene dioxygenase: Side-on binding of dioxygen to iron. Science **299**, 1039 (2003)
30. Jagadeesh, R.V., Surkus, A.-E., Junge, H., Pohl, M.-M., Radnik, J., Rabeah, J., Huan, H., Schünemann, V., Brückner, A., Beller, M.: Nanoscale Fe2O3-based catalysts for selective hydrogenation of nitroarenes to anilines. Science **342**, 1073 (2013)